Research Square

Preprints are preliminary reports that have not undergone peer review.
They should not be considered conclusive, used to inform clinical practice,
or referenced by the media as validated information.

Plant Wax Biomarker Evidence for Late Pleistocene-to-Holocene Forest Resilience and Ecological Refugium Dynamics at Panga ya Saidi, Coastal Kenya

Robert Patalano

rpatalan@bryant.edu

School of Health and Behavioral Sciences, Bryant University https://orcid.org/0000-0002-9075-4556

Jennifer Miller

Center for Social Sciences, Southern University of Science and Technology

Ceri Shipton

McDonald Institute for Archaeological Research

W Carleton

Max Planck Institute of Geoanthropology https://orcid.org/0000-0001-7463-8638

Kasun Gayantha

Department of Biogeochemical Processes, Max Planck Institute for Biogeochemistry

Gerd Gleixner

Max Planck Institute for Biogeochemistry https://orcid.org/0000-0002-4616-0953

Rahab Kinyanjui

MPI-SHH https://orcid.org/0000-0003-2032-8321

Jana Ilgner

Department of Archaeology, Max Planck Institute of Geoanthropology

Emmanuel Ndiema

National Museums of Kenya

Patrick Roberts

Max Planck Institute of Geoanthropology https://orcid.org/0000-0002-4403-7548

Nicole Boivin

Max Planck Institute of Geoanthropology https://orcid.org/0000-0002-7783-4199

Michael Petraglia

Griffith University https://orcid.org/0000-0003-2522-5727

Article

Keywords:

Posted Date: March 6th, 2026

DOI: https://doi.org/10.21203/rs.3.rs-8758549/v1

License: This work is licensed under a Creative Commons Attribution 4.0 International License.
Read Full License

Additional Declarations:
There is **NO** Competing Interest.

Table 1 is available in the Supplementary Files section.

Plant Wax Biomarker Evidence for Late Pleistocene-to-Holocene Forest Resilience and Ecological Refugium Dynamics at Panga ya Saidi, Coastal Kenya

Robert Patalano[1,2], Jennifer M. Miller[2,3], Ceri Shipton[4], W. Christopher Carleton[2], Kasun Gayantha[5], Gerd Gleixner[5], Rahab Kinyanjui[2,6], Jana Ilgner[2,7], Emmanuel Ndiema[6], Patrick Roberts[2,8], Nicole Boivin[2,9,10], Michael Petraglia[10,11, 12]

1. Department of Biological and Biomedical Sciences, School of Health and Behavioral Sciences, Bryant University, Smithfield, Rhode Island, USA.

2. Department of Coevolution of Land Use and Urbanization, Max Planck Institute of Geoanthropology, Jena, Germany.

3. Center for Social Sciences, Southern University of Science and Technology, Shenzhen, Guangdong, China.

4. University College London, Institute of Archaeology, London, United Kingdom.

5. Department of Biogeochemical Processes, Max Planck Institute for Biogeochemistry, Jena, Germany.

6. Department of Earth Sciences, National Museums of Kenya, Nairobi, Kenya.

7. Laboratory and Fieldwork Central Unit, Max Planck Institute of Geoanthropology, Jena, Germany

8. Institute of Prehistoric Archaeology, University of Cologne, Cologne, Germany.

9. School of Social Science, The University of Queensland, Brisbane, Australia.

10. School of Environment and Science, Griffith University, Brisbane, Australia.

11. Australian Research Centre for Human Evolution, Griffith University, Brisbane, Australia.

12. Human Origins Program, Smithsonian Institution, Washington, DC, USA.

Abstract

The role of environmental refugia in human evolutionary ecology is unclear due to a lack of correlated high-resolution datasets linking climate and environmental change with human behavior. Panga ya Saidi, coastal Kenya, is one of the few sites in eastern Africa that has both on-site climate and vegetation proxy archives and an archaeological assemblage that documents the Middle-to-Later Stone Age transition. Here, we present a 57,000-year plant wax biomarker record from Panga ya Saidi's archaeological sediments and evaluate the site's potential as an ecological refugium. Compound specific plant wax carbon ($\delta^{13}C$) and hydrogen ($\delta^{2}H$) isotope data indicate long-term ecological stability and a C_3-dominated ecosystem since at least Marine Isotope Stage (MIS) 3. Despite arid phases, including a hyper-arid Last Glacial Maximum, the tropical moist broadleaf forest biome at Panga ya Saidi persisted through these perturbations, giving humans the

ability to access forest, grassland, and coastal habitats via mobile foraging and social networking. The ecological contrasts between the coastal forest mosaic and surrounding ecoregions likely played a role in deep-time technological developments, with habitat variability and ecological diversity being conducive to cultural innovations regardless of climatic perturbations.

Main

In evolutionary ecology, the term 'refugia' is often used to indicate ecosystems that resist spatial and temporal damages or recover quickly following perturbation or disturbances[1]. This is because these resilient ecosystems have distinct ecological characteristics that isolate them from regional climatic or environmental stress[2]. Refugia have also been discussed in terms of spatial variability and characterized as microhabitats that provide resources to specific biotic communities, including humans, that are not readily available in adjacent, less-resilient ecosystems[3]. Intrinsically, a refugium is an area in which a species' habitat is present throughout a period of instability, supporting populations with varying dispersal abilities and response adaptations to ambient climatic processes[4].

There has been a recent emphasis placed on the importance of stable, or climatically resilient, ecosystems that may have allowed for the long-term development of material culture or engagement with specific resource bases[5-13]. The cultural and lithic assemblages from Panga ya Saidi, coastal Kenya (Fig. 1), have been instrumental for understanding long-term human habitation and resource procurement in a tropical, deciduous forest situated within a larger wooded grassland biome. The Middle-to-Later Stone Age occupation at Panga ya Saidi that spans the last five Marine Isotope Stages (MIS), is one of the few archaeological assemblages in eastern Africa that contains the MSA-to-LSA-to-Iron Age transitions and has both on-site climate and vegetation proxy data[14-16]. Placing human adaptive traits within a local-to-regional environmental framework is now the focus for linking climate and environment changes to the development of the LSA[17]. This is due to the emergence of the LSA in eastern Africa being associated with climate instability and hydroclimate variability[18-21], but also the existence of biogeographic havens[12].

There is increasing evidence across Africa for human habitation of tropical forest biomes throughout the Pleistocene[16,22-26]. Rarely, however, are high-resolution records linking climate and environmental change with human behavior available in these biomes[26]. Panga ya Saidi exhibits the earliest known appearance of the LSA in Africa and is hypothesized to be a Late Pleistocene environmental refugium buffered against dramatic climate shifts[4,14,16]. Therefore, it presents a unique opportunity to test hypotheses on the degree to which eastern African forest biomes may have acted as refugia despite regional or global climate changes and environmental reorganizations.

Here, we present a ~57-thousand-year vegetation and hydroclimate record from carbon and hydrogen isotopes of plant wax *n*-alkanoic acids directly from Panga ya Saidi's archaeological sediments spanning the period from Early MIS 3 to the Iron Age (SI Fig. 1). Biomarker metrices and compound-specific carbon ($\delta^{13}C$) and hydrogen ($\delta^{2}H$) isotope data provide complimentary, but additive, insight into the localized distribution of both C_3 and C_4 plants in response to precipitation variability by building upon existing faunal isotope data[14,16]. We use the isotopically well-defined distribution of C_3 and C_4 plants' $\delta^{13}C$ values to estimate past plant ecology and evaluate $\delta^{2}H$ as a proxy for precipitation to investigate whether Panga ya Saidi acted as an ecological refugium for *H. sapiens*.

Results

Plant Wax Biomarker Preservation and Distribution

Panga ya Saidi is in the Northern Swahili Coastal Forests and Woodlands ecoregion (Fig. 1a). Because the site's easterly facing position on an escarpment ~168 m.a.s.l. protects it from winds coming from the Indian Ocean coastal plain to the east and the elevated semiarid plateaus of the interior to the west, the dominant source of rockshelter sedimentary *n*-alkanoic acids are the tropical moist broadleaf forest species growing directly in and around the site (Supplementary Table 1; SI Fig. 2). Plant wax biomarker distributions are dominated by even-numbered, higher chain lengths indicating a terrestrial plant wax source[27]. All but three samples have C_{30} as the dominant *n*-alkanoic acid (presented as Fatty Acid Methyl Esters, or FAMEs), while the C_{32} and C_{28} homologues are most abundant in two and one sample, respectively. In samples with C_{30} as the most abundant compound, all but one has C_{32} as the second most dominant FAME; the other sample has C_{28} as the second most abundant compound (Fig. 2; Table 1). The relative contributions of C_{28} and C_{32} are negatively correlated (Spearman's rs=0.756), co-varying throughout the sequence (Figure 2e).

The carbon preference index (CPI) of the C_{20}-C_{34} FAMEs ranges between 1.65 and 2.47 (1.88 ± 0.05, n=19) (Fig. 2a). These values are somewhat low for plant-derived CPI values[28], and may indicate that some degradation occurred in the longer chain compounds. However, the wide range of CPI observed in modern African plants (<1 to 99, with 96.0% of all CPI values being greater than or equal to 1; 81.2% greater than or equal to 2; and 60.7% greater than or equal to 5) precludes its use as a single metric on which to base sample integrity[28].

The average chain length ($ACL_{20\text{-}35}$) ranges from 27.98 to 29.90 (29.37 ± 0.41, n=19) (Fig. 2b), consistent with previous reports of ACL from African terrestrial plants[28,29]. Additionally, we measured the submerged/terrestrial ratio (STR_{24}) and the algal/terrestrial ratio ($ATR_{14\text{-}18}$), metrics to differentiate the fatty acids of submerged and terrigenous plants and algae and terrigenous plants, respectively[30]. The STR_{24} ranges between a 0.03 and 0.11 (0.06 ± 0.02, n=10) while the $ATR_{14\text{-}18}$ ranges between 0.22 and 0.60 (0.35 ± 0.10, n=10), both of which indicate a dominant terrestrial plant wax source (Figure 2c, d).

Compound-Specific Carbon Isotope Analysis

The $\delta^{13}C$ data from *n*-alkanoic acids show an unequivocal dominance of C_3 vegetation throughout the Panga ya Saidi depositional sequence with a long-term trend toward ^{13}C-depleted plant waxes (Fig. 3a; Table 1). $\delta^{13}C$ values range between -28.4 ‰ and -32.8 ‰ (-29.9 ± 0.9 ‰, n=57), and when separated by FAME homologue, range between -28.4 ‰ and -30.1 ‰ (C_{28}, -29.1 ± 0.4 ‰, n=19), -29.1 ‰ and -31.2 ‰ (C_{30}, -29.8 ± 0.5 ‰, n=19), and -29.6 ‰ and -32.8 ‰ (C_{32}, -30.7 ± 0.8 ‰, n=19). The C_{32} FAME displayed the lowest, or most negative, $\delta^{13}C$ values in all samples. The C_{28} *n*-acid on the other hand, showed the highest values in all samples, with the largest isotopic variations between C_{28} and C_{32} being -2.8 ‰ in Layers 1/2 (5-7cm). On average, C_{28} has higher $\delta^{13}C$ values by 1.6 ‰ compared to C_{32}, which is expected given that African herbs, shrubs, and trees often exhibit depleted $\delta^{13}C$ values coinciding with increasing chain length[29,31]. Because the C_{28}-C_{32} FAMEs exhibit the same isotopic trends through the column, we report on the weighted average in addition to individual compound $\delta^{13}C$ (Fig. 3a).

Compound-Specific Hydrogen Isotope Analysis

Like the carbon data, the $\delta^{2}H$ record from Panga ya Saidi shows a long-term trend toward lower values through time (Fig. 3b). In contrast to the $\delta^{13}C$ data, there is a major, ~30 ‰, shift to higher

δ^2H values during the LGM. This is followed by a ~40 ‰, shift to lower δ^2H values in the Terminal Pleistocene. Hydrogen isotope measurements for the C_{28}-C_{32} FAMEs range between -132.8 ‰ and -72.1 ‰ (-107.3 ± 12.1 ‰, n=47). When separated by FAME homologue, δ^2H values range between -72.1 ‰ and -126.1‰ (C_{28}, -109.1 ± 11.7 ‰, *n*=19), -82.4 ‰ and -124.4 ‰ (C_{30}, -107.4 ± 10.1 ‰, *n*=19), and -82.1 ‰ and -132.8 ‰ (C_{32}, -103.0 ± 16.3 ‰, *n*=9). The hydrogen isotopic composition of the C_{28} and C_{30} *n*-alkanoic acids are weakly correlated (Spearman's *rs*=0.408), demonstrating that these compounds were derived from a common source and record similar climate processes. We also report on the weighted average in addition to individual compound δ^2H (Fig. 3b).

Discussion

The CPI of the C_{20}-C_{34} FAMEs initially indicates that some samples suffered from biodegradation (Fig. 2a; Table 1), with the site's relatively wet and warm environmental setting likely acting as a catalyst for microbial activity that would have degraded sedimentary organic matter over time[32,33]. Although $CPI_{20\text{-}34}$ values fall within a relatively narrow range (1.65 – 2.47), the plant wax $\delta^{13}C$, and for the most part, δ^2H data follow the same general trend as the site's bulk $\delta^{13}C$ and $\delta^{18}O$ faunal isotope values, respectively[14,16] (Fig. 4; 5). Therefore, we are confident that biodegradation did not impact the isotope values of the C_{28}-C_{32} FAMEs as has been shown elsewhere[34,35].

Relative abundances of plant wax biomarkers have previously been used to determine the proportional sedimentary input of C_3 woody plants and C_3 and C_4 graminoids[28,36]. The C_{30} FAME is dominant in all but 3 of the 19 samples, with 15 of these having C_{32} as the second most prominent compound (Fig. 2e). These distributions show that woody plants were the major ecological component of the region since at least MIS 4 and, if herbs were present, only contributed a small portion of waxes to the archaeological sediments[28,29,37,38].

Average chain length (ACL) is another metric used as a vegetation proxy. $ACL_{20\text{-}34}$ falls between 27.98 to 29.90 (29.37 ± 0.14), attributed to an abundance of woody vegetation. However, the presence of mid-chain homologues (SI Fig. 2) likely represent the biosynthesis of these compounds by non-vascular bryophytes[30,39] favouring high levels of moisture and water pooling. Even today, the high-humidity micro-climate at Panga ya Saidi promotes the growth of a wide variety of plant ecological life-forms (Supplementary Table 1). Therefore, as Panga ya Saidi was heavily wooded and had a consistent water supply and relatively high humidity, the micro-climate throughout both the Pleistocene and Holocene likely fostered the growth of bryophytes and algae on both the ground layer and amongst rocky surfaces of cave walls.

The C_{28}-C_{32} $\delta^{13}C$ data demonstrates a C_3 dominated environment over the past ~57,000 years. Interestingly, this deviates from previously measured bulk $\delta^{13}C$ values[14,16], which show a large contribution of C_4 plants in animal diets (Fig. 4). Although the compound specific isotope record shows relatively higher values in Early to Mid MIS 3, followed by stability through the Terminal Pleistocene, and then a shift towards ^{13}C-depleted values in the Holocene, the faunal isotopes signal more of a mosaic regional environment. That is, the immediate forest environment of Panga ya Saidi (as documented in the biomarker data) was surrounded by more open habitat types like wooded grasslands and grasslands (as documented by faunal data). The bulk $\delta^{13}C$ range of both grazers and browsers indicates that fauna exploited by humans ate a variety of plant foods from tropical forest to open woodland habitats, including C_4 grassland biomes[14]. Meanwhile, the $C_{28\text{-}32}$ FAME $\delta^{13}C$ data demonstrate that the escarpment on which Panga ya Saidi sits has hosted a tropical forest since at least Early MIS 3, likely brought on by more humid conditions and greater rainfall, as indicated by plant wax δ^2H.

Panga ya Saidi's position on an escarpment, that acts as physiographic barrier between the Indian Ocean coastal plain to the east and the elevated semiarid plateaus of the interior to the west, establishes it as a hydrologically unique archaeological site in eastern Africa. Overall, δ^2H values at Panga ya Saidi suggest that MIS 3 was relatively drier than the Terminal Pleistocene and Holocene, with a mean δ^2H difference of ~12 ‰ between the two phases (Figs. 3, 5). Separating these two phases is a comparatively intense dry period marked by a high weighted average δ^2H of -76.7 ± 4.9 ‰, a ~30 ‰, likely reflecting increased global aridity of the LGM. This was then followed by a nearly 40 ‰ decrease in δ^2H in the Terminal Pleistocene. This major excursion is not necessarily observed in other regional records from this region[40,41], nor does it appear to be reflected in the faunal $\delta^{18}O$ data (Fig. 5). Nevertheless, this arid perturbation did not have a significant influence on the overall proportion of C_3 and C_4 plants (i.e., $\delta^{13}C$) directly at Panga ya Saidi (Fig. 4), perhaps indicating that the forest biome surrounding Panga ya Saidi was buffered against, or recovered quickly from, dramatic perturbation or disturbances.

The application of refugia models to the study of human evolutionary ecology is often complicated by the term 'refugia' being somewhat of an intangible concept. Although climatically resilient ecosystems that could support an enduring presence during regional disturbances would have been alluring to Pleistocene human populations[4], identifying such biogeographic havens is difficult without correlated archaeological and paleoecological datasets. The coupled plant wax biomarker and faunal isotope data and archaeological assemblages from Panga ya Saidi bring new insights into the spatiotemporal ecological characteristics of the surrounding Northern Swahili Coastal Forests and Woodlands ecoregion.

Occupations at Panga ya Saidi indicate a persistent human presence from ~78 ka onwards, marking a departure from the overall regional, eastern African pattern of long periods of site abandonment in the Late Pleistocene and Holocene[17,42]. Persistent occupations have been identified by archaeologists as putative refugial zones within Africa[4]. As Panga ya Saidi is under the influence of the Indian Ocean Monsoon, its proximity to the coast, and its geographical setting on an escarpment consisting of dense and taxonomically diverse coastal forest plant species likely enabled long-term habitation[16], which was not necessarily the case at many other Late Pleistocene eastern African sites[43]. This stability would have been advantageous to the development of material culture at Panga ya Saidi during climatically variable episodes when extremely dry conditions caused severe habitat changes and limited resource availability elsewhere in eastern Africa.

Two possibilities underlie the long-term ecological stability at Panga ya Saidi[44]: 1) the coastal forest biome was buffered against arid episodes and 2) local ecology was able to recover quickly once conditions ameliorated. The plant wax data attests to each of these in varying degrees. For example, the $\delta^{13}C$ evidence shows that the Northern Swahili Coastal Forest persisted since at least MIS 3, while δ^2H indicates a relatively humid climate buffered against more arid climate further inland[40,45]. The intense dry period during the LGM and other relatively minor dry phases in Mid MIS 3, the late Terminal Pleistocene, the Early Holocene, and the Iron Age (Fig. 3) attests to arid episodes occurring historically at Panga ya Saidi. The general lack of response in the plant wax $\delta^{13}C$, however, shows that the local plant ecology either did not suffer extensively from these arid phases or was able to recover quickly after disturbances by being resistant to drought in a way similar to other African tropical forests[46-48]. Exhibiting non-linear response attributes to regional climatic drivers[14,16,44,49-52], the ecological setting at Panga ya Saidi would have been able to withstand relatively extreme, at least short-term, climate anomalies, such as mega-droughts that have been suggested to have occurred elsewhere in eastern Africa[46-48,53].

If we consider 'refugia' as ecosystems that resist spatial and temporal damages or recover quickly following perturbation or disturbances[1,2], then the plant wax biomarker data from Panga ya Saidi demonstrate that this tropical, deciduous forest had distinct ecological characteristics that isolated it from regional climatic or environmental impacts. Additionally, the greater, regional Northern Swahili Coastal Forests and Woodlands ecoregion exhibits spatial microhabitat variability that allowed spatially-adaptable biotic communities, specifically *H. sapiens*, to persist in this region despite environmental disturbances. These characteristics would therefore suggest that Panga ya Saidi's enviro-geographic setting was an ecological refugium. Yet, these broad definitions of 'refugia' can theoretically apply to many habitable areas that vary in size and have favorable climate within a region of largely unfavorable climate. Thus, it may be best to evaluate *H. sapiens*' long-term habitation of Panga ya Saidi within a microhabitat variability framework[54] that considers both resilient and less-resilient ecosystems.

The interconnectedness of populations has been proposed as a key feature of the LSA[55,56]. Panga ya Saidi documents the earliest appearance of the LSA in MIS 4 in the form of miniaturized lithics[52] alongside the novel symbolic material culture item of puka shell beads[49]. Here, newly developed technologies could have assisted in resource acquisition in the neighboring ecosystems[14] while cultural materials could be dispersed along the coast and further inland, specifically along humid, gallery forest type corridors[57]. In MIS 3, for instance, backed lithics are found at both Panga ya Saidi and sites in the interior of eastern Africa[52]; in early MIS 2, the ostrich eggshell beads that characterize the LSA in the interior are dominant at Panga ya Saidi, despite them being produced elsewhere[49]; while in the mid-Holocene coastal connections are reflected in both shellfish consumption and the use of marine shell beads[50]. The contrast in plant wax and faunal isotope data shows that the occupants of Panga ya Saidi were making good use of the ecotonal setting of the site, bringing in faunal resources firstly from more open interior environments and later the coast, perhaps to complement the locally abundant plant resources.

The relatively warm and humid Pleistocene environments within this spatially diverse ecoregion produced readily available food resources, incentivizing persistent habitation at Panga ya Saidi. Despite the hyper-arid LGM, plant wax δ^2H exhibits relatively wet conditions since Late MIS 3, with generally uniform precipitation amounts providing dependable freshwater reserves that would have supported rich plant-food resources. This region would have been particularly valuable to hunter-forager communities during phases of ecological instability and regional drying relative to the more uneven resource distributions of environments further inland. The ecological contrasts between the coastal forest mosaic and surrounding ecoregions likely played a role in the deep-time technological developments that archaeologists are detecting across the region, with habitat variability and ecological diversity being conducive to cultural innovations rather than abandonment during times of climatic perturbation[16].

Living at the interface between the coast and the western interior, the inhabitants of Panga ya Saidi were likely players in, and beneficiaries of, the ecoregion's microhabitat variability. The ability to access forest, grassland, and coastal habitats via mobile foraging, social networking, or both, lends Panga ya Saidi an ecotonal character that would have enhanced long-term stability for human populations. Compound-specific biomarkers have allowed us to get detailed insights and perspectives on climatic and environmental variables in this critical refugial setting, as well as the ecological benefits it may have provided in the Late Pleistocene. These dynamics may, additionally, provide important perspectives regarding population interactions along coastal regions and the development of the Later Stone Age, as well as predictions of landscape-level response variability to climate change in eastern Africa following the emergence of *Homo sapiens*.

Methods

Sample Collection

Today, Panga ya Saidi is a partially-open-ceiling cave system in the Dzitsoni Uplands, 15 km from the Nyali Coast of Kenya (Fig. 1). Although its archaeological significance has only recently been demonstrated, it contains the earliest known human burial in Africa[51], the oldest stratified evidence of marine engagement in eastern Africa[50], and an ~80-thousand-year sequence of lithic technological innovations[16,44,52] and material culture traits[49] that encompass the MSA-LSA-Iron Age transitions.

Sediment samples (*n*=20) were collected from the west wall of Trench 8 during the 2020 field season (SI Fig. 1). Using a solvent-cleaned trowel, 1-2 cm of the trench wall was removed to expose a fresh surface. Once the outer surface was removed, sediment was sampled starting at the bottom of the trench in units of ~2×10×10 cm (height × width × depth), with ~5 cm intervals between each sample. Roughly 150 g of sediment was collected for each sample for paleoenvironmental reconstructions.

Plant Biomarker Extraction and Isolation

Dry, homogenized sediments (~20 g) were extracted with a Büchi SpeedExtractor E-916 Pressurized Speed Extractor (PSE) using 9:1 (v/v) Dichloromethane:Methanol at 100 °C and 103 bar (1500 psi) in three, 10-minute cycles at the Max Planck Institute of Geoanthropology (formerly for the Science for Human History), Jena, Germany. Solvent containing the total lipid extract (TLE) was concentrated to ~1 mL using a Büchi Syncore-Plus evaporator and then evaporated to dryness using a steady stream of N_2. The TLE was separated into Neutral, Acid, and Polar fractions by Aminopropyl column chromatography using 4 mL each of 2:1 Dichloromethane:Isopropanol, 4% Acetic Acid in Diethyl Ether, and Methanol, respectively. The Acid fraction was then methylated with 1 mL of 2 % HCl in Methanol at 50 °C for 24 hours to convert *n*-alkanoic acids to Fatty Acid Methyl Esters (FAMEs). The FAMEs were then isolated with 1 mL of 5 % aqueous NaCl and 4 mL Hexane. The Hexane (containing FAMEs) was transferred to new vials and dried with N_2, then the FAMEs were further isolated from other acids using silica gel column chromatography with Hexane and DCM eluents. The DCM fraction containing the FAMEs was characterized with gas chromatography and mass spectrometry.

Molecular Characterization

FAMEs were analyzed with an Agilent 7890B Gas Chromatograph (GC) System equipped with an Agilent HP-5 capillary column (30 m length, 0.25 mm i.d. and 0.25 μm film) coupled to a 5977A Series Mass Selective Detector (MSD) at the Max Planck Institute of Geoanthropology, Jena, Germany. Samples were injected in splitless mode at 250 °C, and the GC oven was programmed from 60 °C (1 min hold) to 150 °C at 10 °C/min, then to 320 °C at 6 °C/min (10 min hold). Helium was the carrier gas with a constant flow of 1.3 mL/min. The MS source was operated at 230 °C with 70 eV ionization energy in the electron ionization (EI) mode and a full scan rate of *m/z* 30-650. The FAMEs were identified by comparing mass spectra and retention times with an in-house, external standard mixture. Abundances are given in uncalibrated intensity units and are intended for comparison as relative values. Relative abundances of the C_{28}-C_{32} FAMEs are presented in Figure 2e.

The average chain length, or the weight-averaged number of FAME compounds, was calculated using the full range of identified compounds (C_{20}-C_{34}) and the following formula:

$$ACL = \frac{20(C_{20}) + 21(C_{21}) + \cdots + 33(C_{33}) + 34(C_{34})}{C_{20} + C_{21} + \cdots + C_{33} + C_{34}}$$

Where C_n is the abundance of the chain length with *n* carbons.

The carbon preference index (CPI), which examines the odd-over-even carbon number predominance and serves as an indicator for hydrocarbon maturity and degradation[58], was calculated using the abundances of odd and even chain lengths from C_{20} to C_{34} and the following formula:

$$CPI = \frac{(C_{20} + C_{22} + \cdots + C_{30} + C_{32}) + (C_{22} + C_{24} + \cdots + C_{32} + C_{34})}{2 \times (C_{21} + C_{23} + \cdots + C_{31} + C_{33})}$$

The submerged/terrestrial ratio (STR), which differentiates fatty acids produced by submerged from terrigenous plants, with terrestrial plants generally having values <0.25[30], was calculated as follows:

$$STR = \frac{C_{24}}{C_{20} + C_{22} + \cdots + C_{32} + C_{34}}$$

The algal/terrestrial ratio (ATR), which differentiates fatty acids produced by algae from terrigenous plants, with terrestrial plants generally having values <0.8[30], was calculated as follows:

$$ATR = \frac{C_{14} + C_{16} + C_{18}}{C_{28} + C_{30} + C_{32} + C_{34}}$$

Spearman's rank test was used to correlate the molecular characterizations of ACL, CPI, and the $\delta^{13}C$ and $\delta^{2}H$ of the individual FAMEs. All tests were run using PAST 4.03123 and an Alpha (α) of 0.05.

Compound Specific Stable Carbon and Hydrogen Isotope Measurements

Compound specific carbon isotope ratios ($\delta^{13}C$) of FAME homologues C_{26}-C_{34} were measured using an Agilent 7890A GC System equipped with an Agilent DB-1MS-UI capillary column (60 m Length, 0.25 mm i.d. and 0.25 μm film), coupled to a Thermo Fisher Scientific Delta V Plus Isotope Ratio Mass Spectrometer at the Max Planck Institute for Biogeochemistry, Jena, Germany. 1 μL samples were injected in splitless mode at 320 °C, and the GC oven was maintained for 1 min at an initial temperature of 110 °C, then increased to 320 °C at 5 °C/min (7 min hold). All samples were measured in triplicates. Helium was the carrier gas with a constant flow maintained at 1.8 mL/min. We report on the C_{28}-C_{32} FAMEs as they were the most abundant in all samples.

Compound specific hydrogen isotope ratios ($\delta^{2}H$) of the C_{26}-C_{34} FAMEs were measured using an Agilent 7890B GC System equipped with an Agilent HP-5 MS capillary column (30 m Length, 0.250 i.d. and 0.25 μm film), coupled to an Elementar Isoprime AnthrovisION Mass Spectrometer by an Elementar GC5 Furnace System Interface operated at 1050 °C at the Max Planck Institute of Geoanthropology. The GC oven was temperature programmed from 60 °C (1

min hold) to 150 °C at 10 °C/min, then to 320 °C at 6 °C/min (10 min hold). Helium was the carrier gas with a constant flow of 1.1 mL/min. High purity Helium gas was introduced as three pulses into the IRMS at the start and end of each sample run to evaluate instrument performance and for standardization of the isotopic analyses. Samples were measured in triplicates. We report on the C_{28}-C_{32} FAMEs as they were the most abundant in all samples, though the δ^2H of the C_{32} FAME was only successfully measured in 9 of 19 samples.

The accuracy of the $\delta^{13}C$ and δ^2H values were evaluated against in-house (C_{31}-C_{33} *n*-alkane, MPI Biogeochemistry) and international (Indiana F8-2, Arndt Schimmelmann, University of Indiana) standard laboratory mixtures injected after every three sample injections. The standard deviation of the C_{14}-C_{20} methyl and ethyl esters and C_{31}-C_{33} *n*-alkanes working standard were ≤0.5 ‰ for $\delta^{13}C$ and ≤7.5 ‰ for δ^2H. Drift corrections were determined by the standards run after every sample. Isotopic ratios are expressed as $\delta^{13}C$ values in per mil (‰) relative to the Vienna Pee Dee Belemnite (VPDB) standard with the following equation:

$$\delta^{13}C = \left(\left(\frac{^{13}C}{^{12}C}Sample \div \frac{^{13}C}{^{12}C}Standard\right) - 1\right) \times 1000$$

δ^2H ratios are also expressed in per mil (‰) but relative to the Vienna Standard Mean Ocean Water (VSMOW) standard and the following equation:

$$\delta^{2}H = \left(\left(\frac{^{2}H}{^{1}H}Sample \div \frac{^{2}H}{^{1}H}Standard\right) - 1\right) \times 1000$$

In addition, the H_3^+ factor was determined daily for δ^2H measurements, having an average value of 3.06 ± 0.06, thus confirming the stability of the analytical system. (The isotope software automatically corrected for H_3 contributions using the H_3^+ factor.)

Corrections were made on the FAMEs to remove the isotopic contribution from the methyl group added during methylation using the following formulas for carbon and hydrogen:

$$\delta^{13}C_{FA} = \frac{(n+1) \times \delta^{13}C_{FAME} + 39.58}{n}$$

Where:

- $\delta^{13}C_{FA}$ represents the $\delta^{13}C$ of the given FA prior to methylation
- $\delta^{13}C_{FAME}$ is the $\delta^{13}C$ value of the measured FAME
- -39.58 (± 0.3) is the $\delta^{13}C$ of the methanol used for preparation of the FAME
- *n* is the number of carbon atoms in the (non-methylated) fatty acid.

$$\delta^{2}H_{FA} = \frac{(2n+2) \times \delta D_{FAME} + 71.8 \times 3}{2n-1}$$

Where:

- δ^2H_{FA} represents the δ^2H of the given FA prior to methylation
- δ^2H_{FAME} is the δ^2H value of the measured FAME
- -71.8 (± 1.6) is the δ^2H of the methanol used for preparation of the FAME

- n is the number of carbon molecules in the (non-methylated) fatty acid.

Dates and Bayesian Modelling

Our age model is constrained using Bayesian modelled radiocarbon and optically stimulated luminescence ages for the stratigraphic sequence[59]. We used the Bchronology algorithm from the R package “"Bchron” to create an age-depth model for Panga ya Saidi. The algorithm is based on a Poisson-Gamma model for sediment accumulation. The model assumes the sedimentation process is monotone (always increasing or paused but never decreasing) and that the deposition rate can change between a given set of chronological tie-points. The tie-points consist of dated sediment layers between which the model interpolates the age-depth relationship for any desired set of depths, in this case, the boundaries between stratigraphic layers.

References

1 Sedell, J. R., Reeves, G. H., Hauer, F. R., Stanford, J. A. & Hawkins, C. P. Role of refugia in recovery from disturbances: Modern fragmented and disconnected river systems. *Environmental Management* **14**, 711-724, doi:10.1007/BF02394720 (1990).

2 Davis, J., Pavlova, A., Thompson, R. & Sunnucks, P. Evolutionary refugia and ecological refuges: key concepts for conserving Australian arid zone freshwater biodiversity under climate change. *Global Change Biology* **19**, 1970-1984, doi:https://doi.org/10.1111/gcb.12203 (2013).

3 Patalano, R. *et al.* Ecological stability of Late Pleistocene-to-Holocene Lesotho, southern Africa, facilitated human upland habitation. *Communications Earth & Environment* **4**, 129, doi:10.1038/s43247-023-00784-8 (2023).

4 Blinkhorn, J., Timbrell, L., Grove, M. & Scerri, E. M. L. Evaluating refugia in recent human evolution in Africa. *Philosophical Transactions of the Royal Society B: Biological Sciences* **377**, 20200485, doi:doi:10.1098/rstb.2020.0485 (2022).

5 Burrough, S. L., Thomas, D. S. G. & Barham, L. S. Implications of a new chronology for the interpretation of the Middle and Later Stone Age of the upper Zambezi Valley. *Journal of Archaeological Science: Reports* **23**, 376-389, doi:https://doi.org/10.1016/j.jasrep.2018.10.016 (2019).

6 Shea, J. The Middle Stone Age archaeology of the Lower Omo Valley Kibish Formation: excavations, lithic assemblages, and inferred patterns of early *Homo sapiens* behavior. *Journal of Human Evolution* **55**, 488-485 (2008).

7 Leplongeon, A. The Main Nile Valley at the End of the Pleistocene (28–15 ka): Dispersal Corridor or Environmental Refugium? *Frontiers in Earth Science* **8**, doi:10.3389/feart.2020.607183 (2021).

8 Ossendorf, G. *et al.* Middle Stone Age foragers resided in high elevations of the glaciated Bale Mountains, Ethiopia. *Science* **365**, 583-587, doi:doi:10.1126/science.aaw8942 (2019).

9 Brandt, S. A. *et al.* Early MIS 3 occupation of Mochena Borago Rockshelter, Southwest Ethiopian Highlands: Implications for Late Pleistocene archaeology, paleoenvironments and modern human dispersals. *Quaternary International* **274**, 38-54, doi:https://doi.org/10.1016/j.quaint.2012.03.047 (2012).

10 Pazan, K. R., Dewar, G. & Stewart, B. A. The MIS 5a (~ 80 ka) Middle Stone Age lithic assemblages from Melikane Rockshelter, Lesotho: Highland adaptation and social fragmentation. *Quaternary International* **611-612**, 115-133, doi:https://doi.org/10.1016/j.quaint.2020.11.046 (2022).

11 Stewart, B. A., Parker, A. G., Dewar, G., Morley, M. W. & Allott, L. F. in *Africa from MIS 6-2: Population Dynamics and Paleoenvironments* (eds Sacha C. Jones & Brian A. Stewart) 247-271 (Springer Netherlands, 2016).

12 Bushozi, P. M., Skinner, A. & de Luque, L. The Middle Stone Age (MSA) Technological Patterns, Innovations, and Behavioral Changes at Bed VIA of Mumba Rockshelter, Northern Tanzania. *African Archaeological Review* **37**, 293-310, doi:10.1007/s10437-019-09360-y (2020).

13 Blinkhorn, J. & Grove, M. The structure of the Middle Stone Age of eastern Africa. *Quaternary Science Reviews* **195**, 1-20, doi:https://doi.org/10.1016/j.quascirev.2018.07.011 (2018).

14 Roberts, P. *et al.* Late Pleistocene to Holocene human palaeoecology in the tropical environments of coastal eastern Africa. *Palaeogeography, Palaeoclimatology, Palaeoecology* **537**, 109438, doi:https://doi.org/10.1016/j.palaeo.2019.109438 (2020).
15 Mercader, J. *et al.* Phytolith Palaeoenvironments at Mumba Rock Shelter. *Frontiers in Ecology and Evolution* **9**, doi:10.3389/fevo.2021.699609 (2021).
16 Shipton, C. *et al.* 78,000-year-old record of Middle and Later Stone Age innovation in an East African tropical forest. *Nature Communications* **9**, doi:10.1038/s41467-018-04057-3 (2018).
17 Timbrell, L., Grove, M., Manica, A., Rucina, S. & Blinkhorn, J. A spatiotemporally explicit paleoenvironmental framework for the Middle Stone Age of eastern Africa. *Scientific Reports* **12**, 3689, doi:10.1038/s41598-022-07742-y (2022).
18 McBrearty, S. & Brooks, A. The Revolution That Wasn't: A New Interpretation of the Origin of Modern Human Behavior. *Journal of Human Evolution* **39**, 453-563 (2000).
19 Blome, M., Cohen, A., Tryon, C. & Brooks, A. The environmental context for the origins of modern human diversity: a synthesis of regional variability in African climate 150,000-30,000 years ago. *Journal of Human Evolution* **62**, 563-592 (2012).
20 Eren, M. I., Diez-Martin, F. & Dominguez-Rodrigo, M. An empirical test of the relative frequency of bipolar reduction in Beds VI, V, and III at Mumba Rockshelter, Tanzania: implications for the East African Middle to Late Stone Age transition. *Journal of Archaeological Science* **40**, 248-256, doi:https://doi.org/10.1016/j.jas.2012.08.012 (2013).
21 Cohen, A. *et al.* Ecological consequences of early late Pleistocene megadroughts in tropical Africa. *Proceedings of the National Academy of Sciences of the United States of America* **104**, 16422-16427 (2007).
22 Mercader, J. Forest people: the role of African rainforests in human evolution and dispersal. *Evolutionary Anthropology* **11**, 117-124 (2002).
23 Mercader, J. in *Under the Canopy: The Archaeology of Tropical Rainforests* (ed J Mercader) 1-31 (Rutgers University Press, 2003).
24 Mercader, J. & Brooks, A. S. Long term settlement of lowland tropical rainforests: the evidence from Ituri, D.R. Congo. *Journal of Human Evolution* **34**, A14-A15 (1998).
25 Mercader, J., Marti, R., Gonzalez, I., Sanchez, A. & Garcia, P. Archaeological site formation in tropical forests: insights from the Ituri rock shelters, Congo. *Journal of Archaeological Science* **30**, 45-65 (2003).
26 Ben Arous, E. *et al.* Humans in Africa's wet tropical forests 150 thousand years ago. *Nature*, doi:10.1038/s41586-025-08613-y (2025).
27 Patalano, R., Roberts, P., Boivin, N., Petraglia, M. D. & Mercader, J. Plant wax biomarkers in human evolutionary studies. *Evolutionary Anthropology: Issues, News, and Reviews* **n/a**, doi:https://doi.org/10.1002/evan.21921 (2021).
28 Bush, R. T. & McInerney, F. A. Leaf wax *n*-alkane distributions in and across modern plants: Implications for paleoecology and chemotaxonomy. *Geochimica et Cosmochimica Acta* **117**, 161-179 (2013).
29 Vogts, A., Moossen, H., Rommerskirchen, F. & Rullkötter, J. Distribution patterns and stable carbon isotopic composition of alkanes and alkan-1-ols from plant waxes of African rain forest and savanna C_3 species. *Organic Geochemistry* **40**, 1037-1054 (2009).
30 Liu, H. & Liu, W. Concentration and distributions of fatty acids in algae, submerged plants and terrestrial plants from the northeastern Tibetan Plateau. *Organic Geochemistry* **113**, 17-26, doi:doi.org/10.1016/j.orggeochem.2017.08.008 (2017).

31 Garcin, Y. *et al.* Reconstructing C_3 and C_4 vegetation cover using *n*-alkane carbon isotope ratios in recent lake sediments from Cameroon, Western Central Africa. *Geochimica et Cosmochimica Acta* **142**, 482–500 (2014).
32 Brittingham, A., Hren, M. T. & Hartman, G. Microbial alteration of the hydrogen and carbon isotopic composition of *n*-alkanes in sediments. *Organic Geochemistry* **107**, 1-8 (2017).
33 Leahy, J. G. & Colwell, R. R. Microbial degradation of hydrocarbons in the environment. *Microbiological Reviews* **54**, 305-315 (1990).
34 Wu, M. S., West, A. J. & Feakins, S. J. Tropical soil profiles reveal the fate of plant wax biomarkers during soil storage. *Organic Geochemistry* **128**, 1-15 (2019).
35 Nguyen Tu, T. T., Derenne, S., Largeau, C., Bardoux, G. & Mariotti, A. Diagenesis effects on specific carbon isotope composition of plant *n*-alkanes. *Organic Geochemistry* **35**, 317-329 (2004).
36 Tweedy, R. R. *et al.* African C3 grass n-alkane distributions & plant chemotaxonomy. *Organic Geochemistry* **208**, 104994, doi:https://doi.org/10.1016/j.orggeochem.2025.104994 (2025).
37 Rommerskirchen, F., Plader, A., Eglinton, G., Chikaraishi, Y. & Rullkötter, J. Chemotaxonomic significance of distribution and stable carbon isotopic composition of long-chain alkanes and alkan-1-ols in C_4 grass waxes. *Organic Geochemistry* **37**, 1303-1332 (2006).
38 Wang, Y. V. *et al.* What does leaf wax δD from a mixed C3/C4 vegetation region tell us? *Geochimica et Cosmochimica Acta* **111**, 128-139, doi:https://doi.org/10.1016/j.gca.2012.10.016 (2013).
39 Bakkelund, A., Porter, T. J., Froese, D. & Feakins, S. J. Net fractionation of hydrogen isotopes in *n*-alkanoic acids from soils in the northern boreal forest. *Organic Geochemistry* **125**, 1-13 (2018).
40 Tierney, J. E. & deMenocal, P. B. Abrupt shifts in Horn of Africa hydroclimate since the Last Glacial Maximum. *Science* **342**, 843-846 (2013).
41 Tierney, J. E., deMenocal, P. B. & Zander, P. D. A climatic context for the out-of-Africa migration. *Geology* **45**, 1023-1026 (2017).
42 Tryon, C. A. & Faith, J. T. Variability in the Middle Stone Age of Eastern Africa. *Current Anthropology* **54**, S234-S254, doi:10.1086/673752 (2013).
43 Faith, J. T. *et al.* Rethinking the ecological drivers of hominin evolution. *Trends in Ecology & Evolution* **36**, 797-807, doi:10.1016/j.tree.2021.04.011 (2021).
44 Goldstein, S. T. *et al.* Hunter-gatherer technological organization and responses to Holocene climate change in coastal, lakeshore, and grassland ecologies of eastern Africa. *Quaternary Science Reviews* **280**, 1-21, doi:https://doi.org/10.1016/j.quascirev.2022.107390 (2022).
45 Tierney, J. E., Russell, J. M., Sinninghe Damsté, J. S., Huang, Y. & Verschuren, D. Late Quaternary behavior of the East African monsoon and the importance of the Congo Air Boundary. *Quaternary Science Reviews* **30**, 798-807, doi:https://doi.org/10.1016/j.quascirev.2011.01.017 (2011).
46 Bennett, A. C. *et al.* Resistance of African tropical forests to an extreme climate anomaly. *Proceedings of the National Academy of Sciences* **118**, e2003169118, doi:10.1073/pnas.2003169118 (2021).

47 Cole, L. E. S., Bhagwat, S. A. & Willis, K. J. Recovery and resilience of tropical forests after disturbance. *Nature Communications* **5**, 3906, doi:10.1038/ncomms4906 (2014).
48 Willis, K. J., Bennett, K. D., Burrough, S. L., Macias-Fauria, M. & Tovar, C. Determining the response of African biota to climate change: using the past to model the future. *Philos Trans R Soc Lond B Biol Sci* **368**, 20120491-20120491, doi:10.1098/rstb.2012.0491 (2013).
49 d'Errico, F. *et al.* Trajectories of cultural innovation from the Middle to Later Stone Age in Eastern Africa: Personal ornaments, bone artifacts, and ocher from Panga ya Saidi, Kenya. *Journal of Human Evolution* **141**, 102737, doi:https://doi.org/10.1016/j.jhevol.2019.102737 (2020).
50 Faulkner, P. *et al.* 67,000 years of coastal engagement at Panga ya Saidi, eastern Africa. *PLoS ONE* **16**, doi:https://doi.org/10.1371/journal.pone.0256761 (2021).
51 Martinón-Torres, M. *et al.* Earliest known human burial in Africa. *Nature* **593**, 95-100, doi:10.1038/s41586-021-03457-8 (2021).
52 Shipton, C. *et al.* The Middle to Later Stone Age transition at Panga ya Saidi, in the tropical coastal forest of eastern Africa. *Journal of Human Evolution* **153**, 102954, doi:https://doi.org/10.1016/j.jhevol.2021.102954 (2021).
53 Scholz, C. A. *et al.* East African megadroughts between 135 and 75 thousand years ago and bearing on early-modern human origins. *Proceedings of the National Academy of Sciences* **104**, 16416-16421 (2007).
54 Patalano, R. *et al.* Microhabitat Variability in Human Evolution. *Frontiers in Earth Science* **9**, doi:10.3389/feart.2021.787669 (2021).
55 Ambrose, S. in *Thinking small: global perspectives on microlithization* (eds R. Elston & S. Kuhn) 1-29 (AAA, 2002).
56 Shipton, C. Miniaturization and abstraction in the Later Stone Age. *Biological Theory* **18**, 253-268, doi:https://doi.org/10.1007/s13752-022-00423-z (2023).
57 Joordens, J. C. A., Feibel, C., Vonhof, H., Schulp, A. S. & Kroon, D. Relevance of the eastern African coastal forest for early hominin biogeography. *Journal of Human Evolution* **131**, 176-202, doi:https://doi.org/10.1016/j.jhevol.2019.03.012 (2019).
58 Duan, Y. & Xu, L. Distributions of *n*-alkanes and their hydrogen isotopic composition in plants from Lake Qinghai (China) and the surrounding area. *Applied Geochemistry* **27**, 806-814 (2012).
59 Miller, J. M. *et al.* Cave Morphology and Human-Mediated Sediment Deposition: The Evolution of the Cave Floor in panga ya Saidi (coastal Kenya) since the Late Pleistocene. (In Review).

Acknowledgements

RP, JMM, JI, WCC, KG, GG, PR, and MP would like to thank the Max Planck Society for financial support. Portions of laboratory analyses were funded by the European Research Council Starter Grant PANTROPOCENE (no. 850709) awarded to PR. Additional funding was provided by the Sealinks project under a European Research Council 1203 (ERC) grant (no. 206148) (awarded to NB). Research permits for this project was granted by the National Council for Research and Technology (NACOSTI) through affiliation with the National Museums of Kenya, Nairobi. Permission to conduct the research was granted by the Office of the President of the Republic of Kenya through affiliation with the National Museums of Kenya. We thank Gedeon Ashoka and family for permission to excavate at Panga ya Saidi and Mathias Ngonyo for conducting the botanical survey. A particular debt is owed to everyone who participated in the excavations and sample collection. CS would like to thank the McDonald Institute for Archaeological Research (University of Cambridge) and the British Institute in Eastern Africa for additional support. Finally, we gratefully acknowledge constructive feedback provided by our anonymous peer reviewers.

Figure Legends

Figure 1. Location of the Panga ya Saidi archaeological site in coastal Kenya**. 1a.** Ecoregions of the Afrotropic biorealm of southern Kenya and northern Tanzania: 1) Northern Swahili Coastal Forests and Woodlands; 2) Northern *Acacia-Commiphora* bushlands and thickets; 3) East African montane moorlands; 4) East African montane forests; 5) Southern *Acacia-Commiphora* bushlands and thickets; 6) Eastern Arc forests; 7) Zambezian flooded grasslands. **1b.** Terrain of the Indian Ocean coastal plain and the Dzitsoni Uplands escarpment that separates the coastal plain from the semiarid plateaus of the interior to the west. **1c.** Exaggerated elevation profile of transect A-A_1 from the Indian Ocean to the Dzitsoni Uplands.

Figure 2. Plant wax biomarker metrics plotted against sample depth with the boundaries of the Marine Isotope sub-Stages labeled. **2a.** Carbon preference index (CPI); **2b.** Average chain length (ACL); **2c.** Submerged/terrestrial ratio (STR); **2d.** Algal/terrestrial ratio (ATR); and **2e**. relative abundances of the $C_{28\text{-}32}$ FAMEs. See Methods for molecular characterizations and calculations. Sub-categorization of the Marine Isotope Stages (MIS) follows those in Roberts et al., 2019.

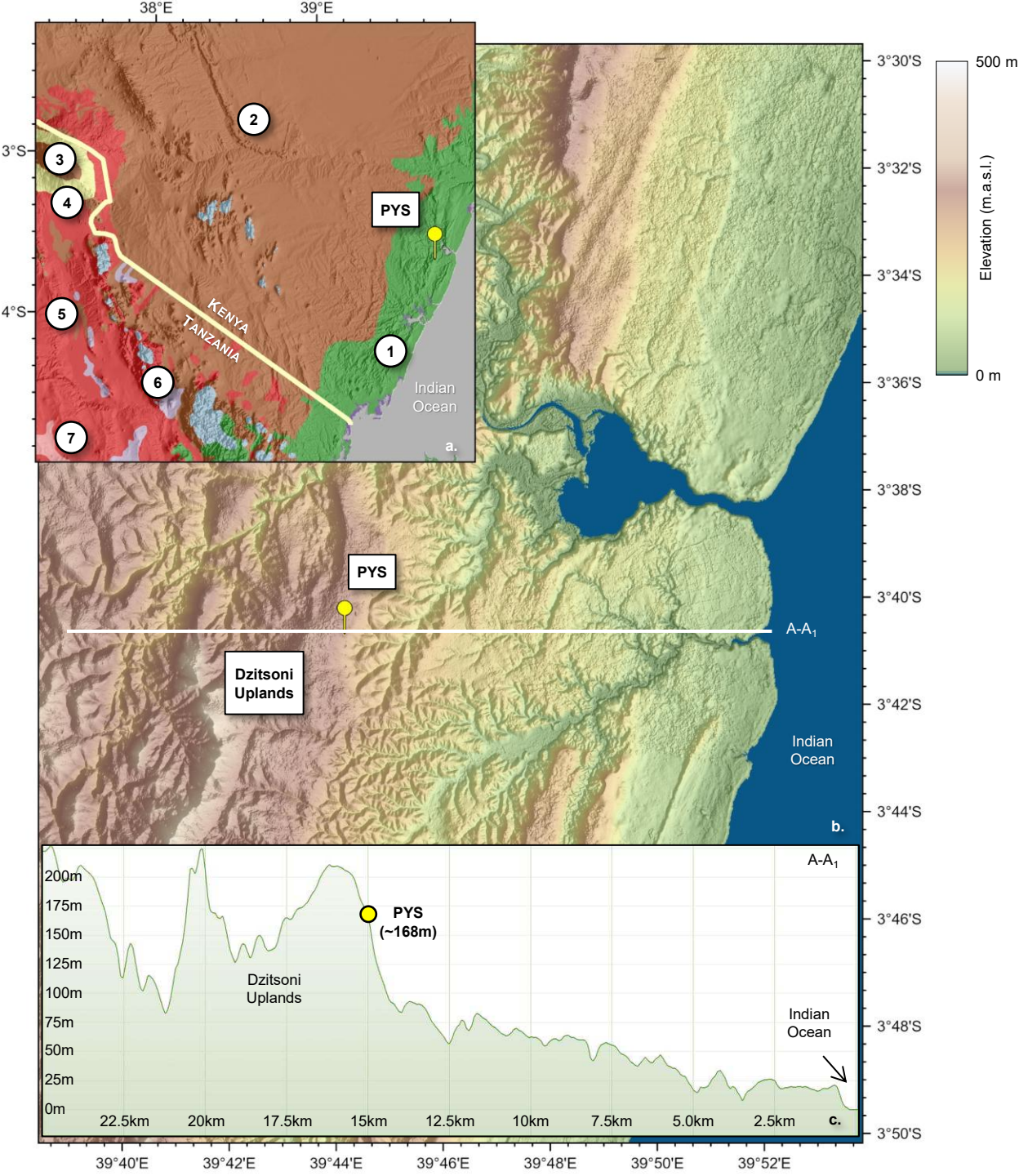
Figure 3. Isotopic ratios of Panga ya Saidi archaeological sediment samples plotted against sample depth with the boundaries of the Marine Isotope Stages (MIS) sub-stages labeled. **3a.** $C_{28\text{-}32}$ FAME and weighted-average $\delta^{13}C$ values; **3b.** $C_{28\text{-}32}$ FAME and weighted-average $\delta^{2}H$ values. Sub-categorization of the Marine Isotope Stages (MIS) follows those in Roberts et al., 2019.

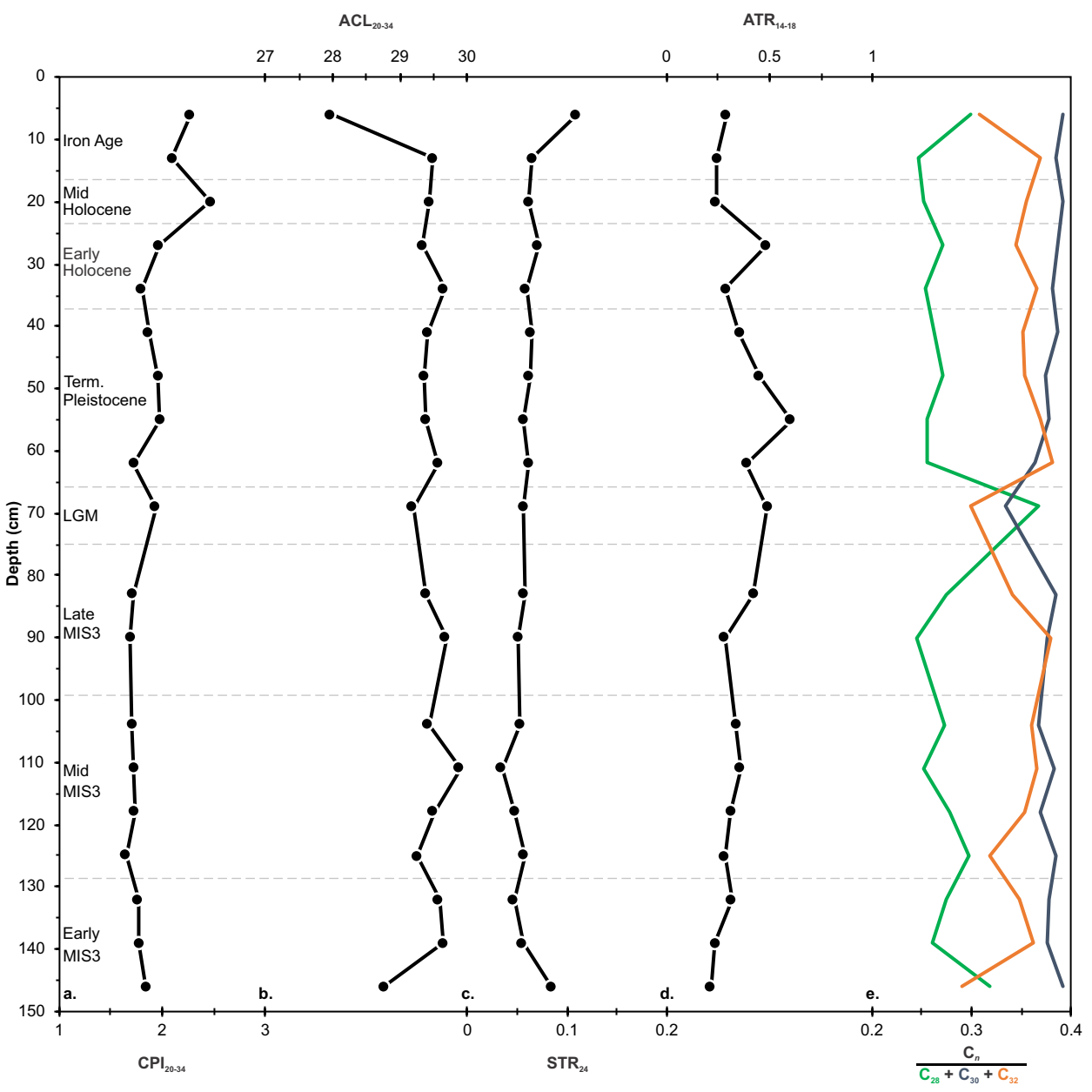
Figure 4. Compound-specific and bulk carbon isotope signatures by Marine Isotope sub-Stage from both plant wax and faunal. **4a.** $C_{28\text{-}32}$ FAME $\delta^{13}C$; **4b.** Bulk $\delta^{13}C$ from faunal specimens classified as grazers; **4c.** Bulk $\delta^{13}C$ from faunal specimens classified as browsers. Bulk data from[13,15].

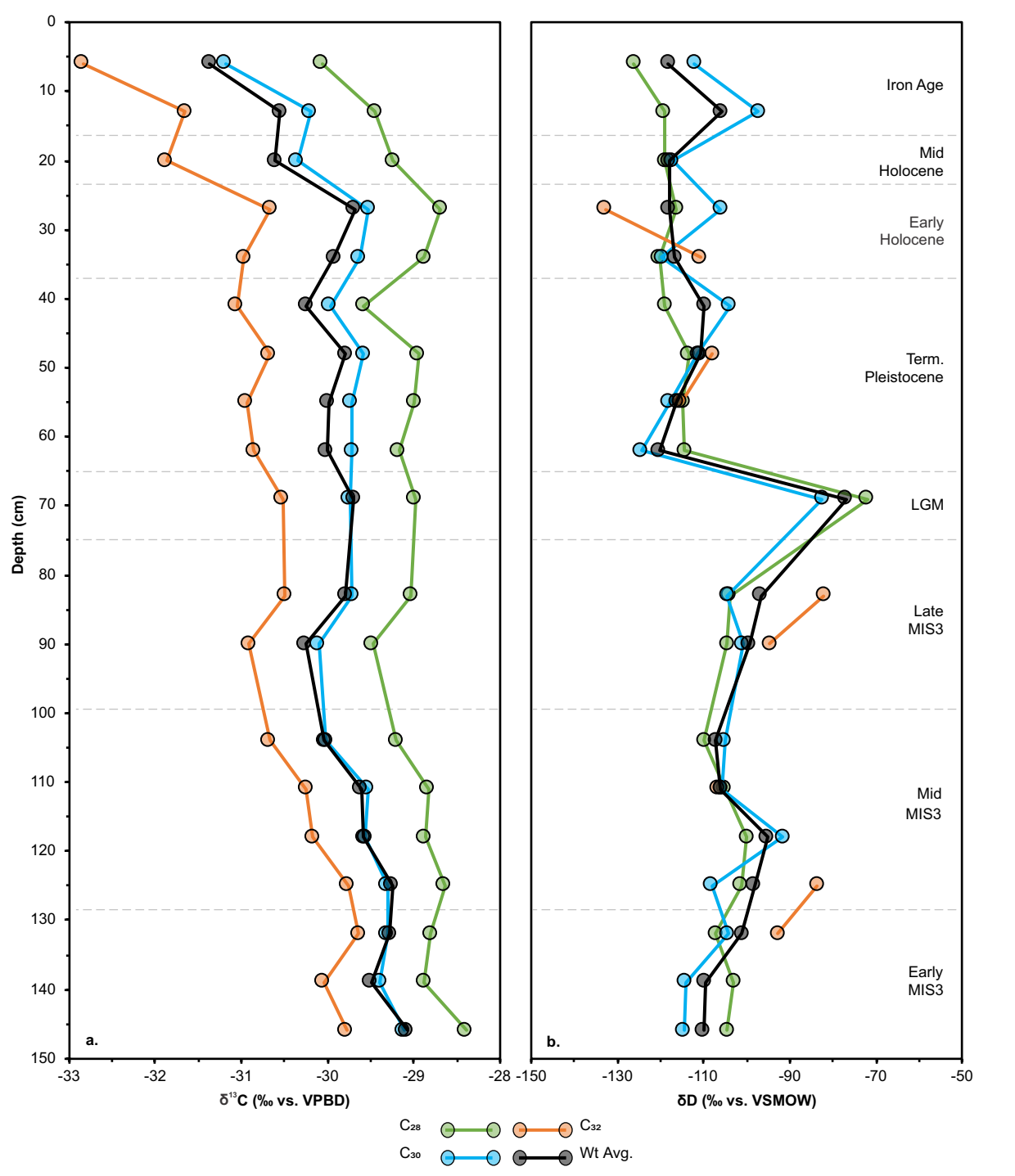
Figure 5. Compound-specific hydrogen and bulk oxygen isotope signatures by Marine Isotope sub-Stage from both plant wax and faunal samples. **4a.** $C_{28\text{-}32}$ FAME $\delta^{2}H$; **4b.** Bulk $\delta^{18}O$ from faunal specimens classified as grazers; **4c.** Bulk $\delta^{18}O$ from faunal specimens classified as browsers. Bulk data from[13,15].

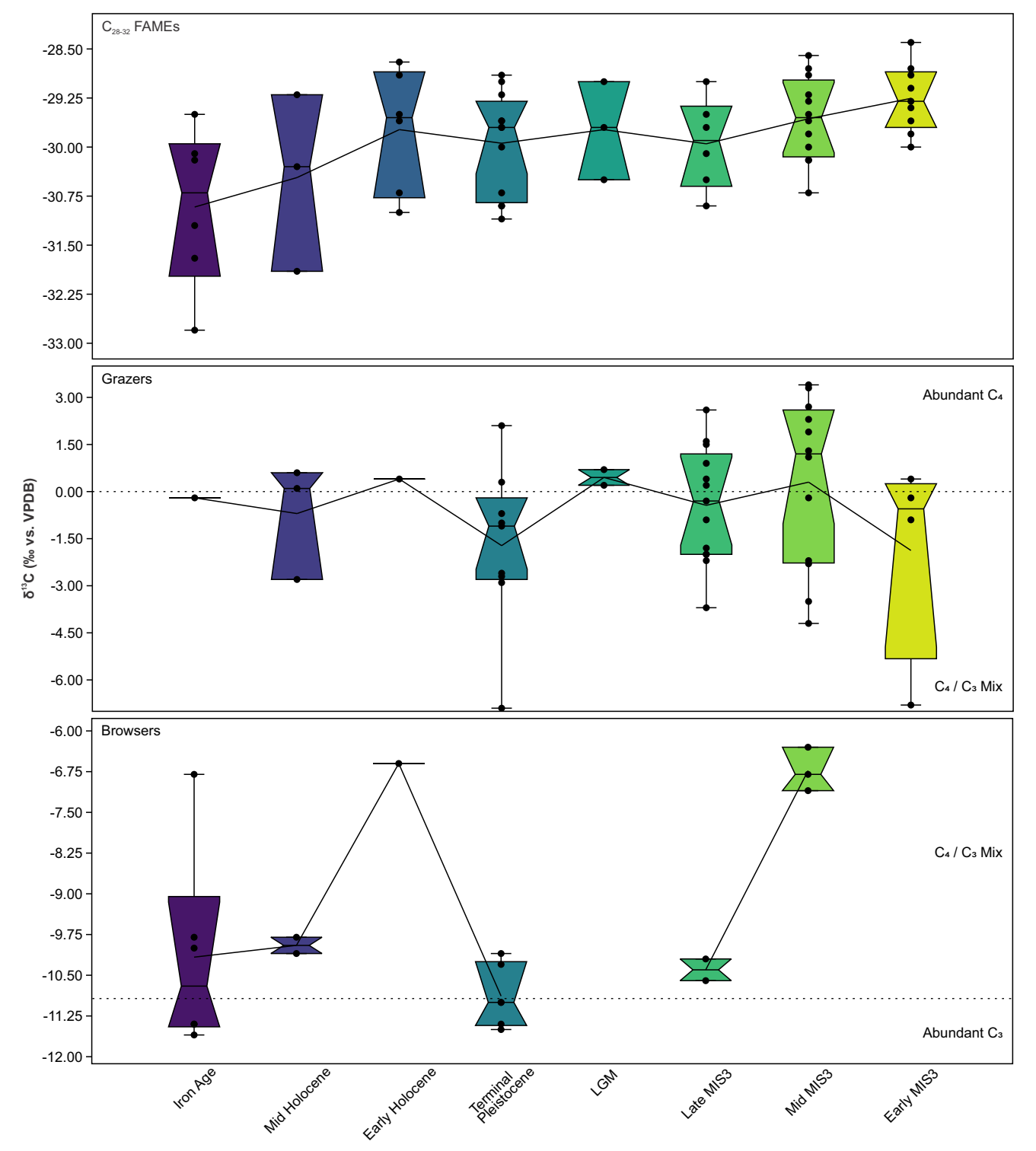
SI Figure 1. Stratigraphic sequence and chronology of Trench 8 at Panga ya Saidi following those first published in Shipton et al., 2018 (reference 16 in main manuscript). Bayesian modeled ages are based on those published in Miller et al., (In Review) (reference 59 in main manuscript). Sub-categorization of the Marine Isotope Stages (MIS) follows those in Roberts et al., 2019 (reference 14 in main manuscript).

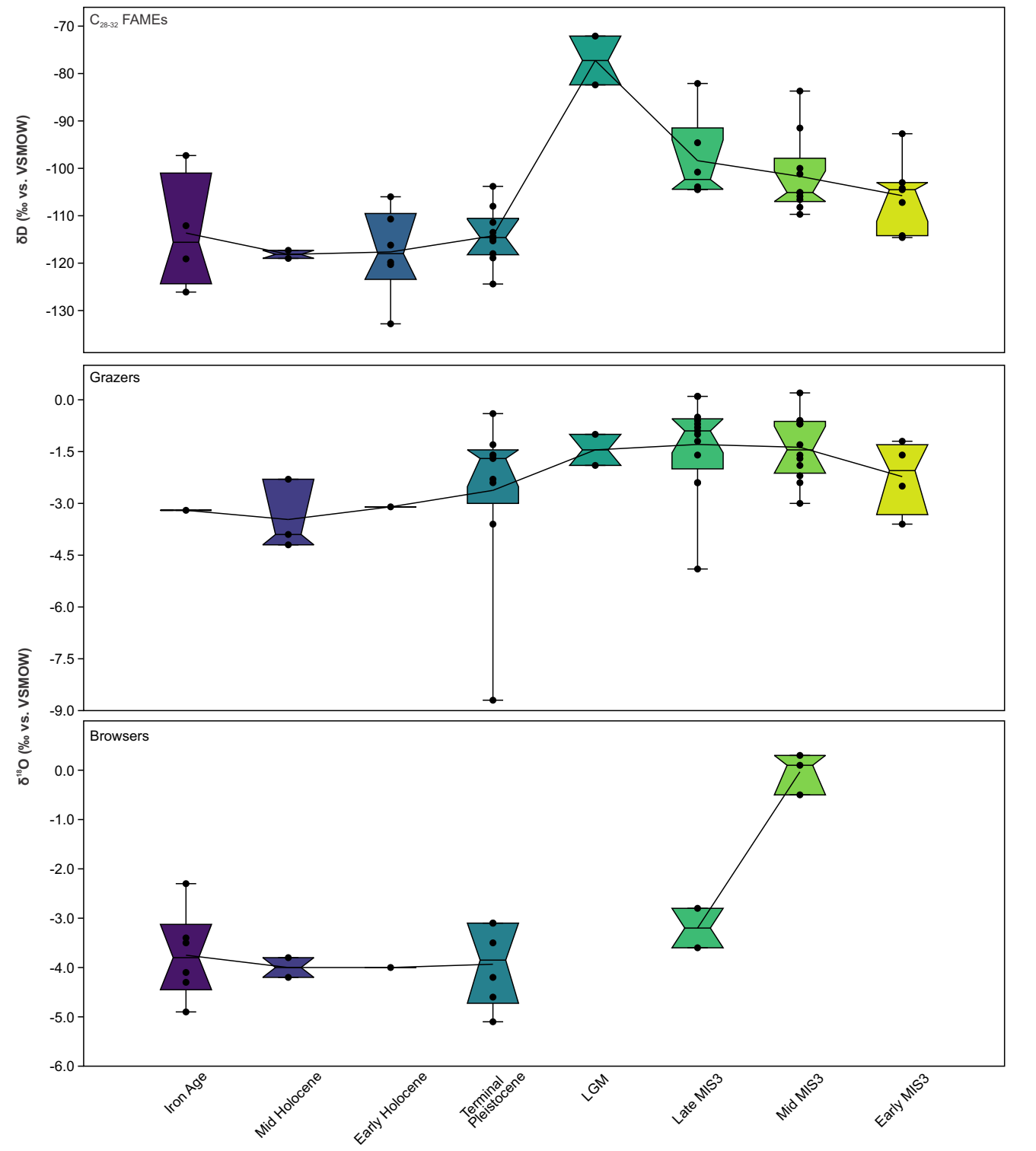
SI Figure 2. Generally, short-chain homologues (e.g., C_{14}-C_{20} *n*-alkanoic acids) characterize aquatic algae, mid-chain homologues (C_{20}-C_{26} *n*-alkanoic acids) characterize submerged and floating aquatic macrophytes and some terrestrial bryophytes, and long-chain homologues (C_{26}-C_{34} *n*-alkanoic acids) characterize terrestrial vegetation (Patalano et al., 2021 (reference 27 in main manuscript)). The dominant source of Panga ya Saidi sedimentary *n*-alkanoic acids are the tropical moist broadleaf forest species growing directly in and around the site (Supplementary Table 1). The presence of mid-chain homologues likely represents the biosynthesis of these compounds by non-vascular bryophytes rather than aquatic macrophytes, as the values from the submerged/terrestrial ratio (STR), which differentiates fatty acids produced by submerged from terrigenous plants, indicate a dominant terrestrial plant wax source.


38°E
39°E
3°S
4°S
2
3
4
5
6
7
1
PYS
KENYA
TANZANIA
Indian Ocean
a.
500 m
Elevation (m.a.s.l.)
0 m
3°30'S
3°32'S
3°34'S
3°36'S
3°38'S
3°40'S
3°42'S
3°44'S
3°46'S
3°48'S
3°50'S
PYS
A-A1
Dzitsoni Uplands
Indian Ocean
b.
A-A1
200m
175m
150m
125m
100m
75m
50m
25m
0m
PYS (~168m)
Dzitsoni Uplands
Indian Ocean
22.5km
20km
17.5km
15km
12.5km
10km
7.5km
5.0km
2.5km
c.
39°40'E
39°42'E
39°44'E
39°46'E
39°48'E
39°50'E
39°52'E


ACL20-34
27
28
29
30
ATR14-18
0
0.5
1
Depth (cm)
0
10
20
30
40
50
60
70
80
90
100
110
120
130
140
150
Iron Age
Mid Holocene
Early Holocene
Term. Pleistocene
LGM
Late MIS3
Mid MIS3
Early MIS3
a.
b.
c.
d.
e.
1
2
3
0
0.1
0.2
0.2
0.3
0.4
CPI20-34
STR24
Cn
C28 + C30 + C32


Depth (cm)
0
10
20
30
40
50
60
70
80
90
100
110
120
130
140
150
a.
-33
-32
-31
-30
-29
-28
δ13C (‰ vs. VPBD)
b.
-150
-130
-110
-90
-70
-50
δD (‰ vs. VSMOW)
Iron Age
Mid Holocene
Early Holocene
Term. Pleistocene
LGM
Late MIS3
Mid MIS3
Early MIS3
C28
C30
C32
Wt Avg.


C28-32 FAMEs
-28.50
-29.25
-30.00
-30.75
-31.50
-32.25
-33.00
Grazers
Abundant C4
C4 / C3 Mix
δ13C (‰ vs. VPDB)
3.00
1.50
0.00
-1.50
-3.00
-4.50
-6.00
Browsers
C4 / C3 Mix
Abundant C3
-6.00
-6.75
-7.50
-8.25
-9.00
-9.75
-10.50
-11.25
-12.00
Iron Age
Mid Holocene
Early Holocene
Terminal Pleistocene
LGM
Late MIS3
Mid MIS3
Early MIS3


C28-32 FAMEs
δD (‰ vs. VSMOW)
-70
-80
-90
-100
-110
-120
-130
Grazers
δ18O (‰ vs. VSMOW)
0.0
-1.5
-3.0
-4.5
-6.0
-7.5
-9.0
Browsers
0.0
-1.0
-2.0
-3.0
-4.0
-5.0
-6.0
Iron Age
Mid Holocene
Early Holocene
Terminal Pleistocene
LGM
Late MIS3
Mid MIS3
Early MIS3

Supplementary Files

This is a list of supplementary files associated with this preprint. Click to download.

- Table1.xlsx
- SITable1.xlsx
- SIFigure2.pdf
- SIFigure1.pdf